# Phase Analysis in the Fe$_2$O$_3$–NiO Mixed Oxides Prepared by Co-Precipitation

S. RAJENDRAN AND V. SITAKARA RAO*

*Department of Chemistry, Indian Institute of Technology, Kharagpur-721302, India*

AND H. S. MAITI

*Materials Science Center, Indian Institute of Technology, Kharagpur-721302, India*

Iron–nickel mixed oxides containing up to 10 mole% of NiO have been prepared by hydroxide co-precipitation technique. The oxide samples have been heated to different temperatures ranging from 300 to 1300°C and studied by infrared spectroscopy, magnetic susceptibility, and X-ray diffraction measurements. The maximum solubility of NiO in Fe$_2$O$_3$ under the present experimental conditions is found to be 2 mole% when the samples are heated to 550°C. The solubility decreases with increase of sintering temperature and also as the total NiO content of the sample increases. Formation of nickel ferrite phase at concentrations higher than 2 mole% of NiO is clearly indicated.

## Introduction

Oxides and oxyhydroxides of iron are of great industrial importance and are widespread in nature. $\alpha$-Fe$_2$O$_3$ is the representative of the transition metal oxides and its electrical, optical, catalytic, and magnetic properties have been studied extensively over the years (1–7). Doping with other metal oxides changes the properties of this oxide quite significantly. For example, $\alpha$-Fe$_2$O$_3$ is not a selective oxidation catalyst but many of its mixed oxides are known to be very effective for certain selective oxidation reactions (8–11). Isomorphous replacement of iron by other metal ions can be easily achieved and the introduction of

higher or lower valent atoms should produce a mixed valent state. The valence of the doping atom greatly affects the solubility and reactivity between reactants. Cr$_2$O$_3$ (12) forms a whole range of solubility with Fe$_2$O$_3$ whereas other oxides like Al$_2$O$_3$, TiO$_2$, SiO$_2$, GeO$_2$, and divalent oxides like MgO, CaO, etc. have only a limited solubility in $\alpha$-Fe$_2$O$_3$ (13–17). The extent of solubility also depends on the experimental conditions. Irrespective of the ionic radius of the metal ions compared to that of Fe$^{3+}$ ions the solubility of the divalent metal ions generally is very low and in most of the cases the formation of corresponding ferrite phase has been reported even with 1 or 2 mole% of the oxides (14, 15, 17). The ionic radius of the Ni$^{2+}$ ion is found to be very close to that of Fe$^{3+}$ ion when both are in

* To whom correspondence is to be addressed.

227

TABLE I

COMPOSITION OF THE SAMPLES

| Code | Concentration of NiO (mole%) | Code | Concentration of NiO (mole%) |
|------|------|------|------|
| FN0 | 0 | FN5 | 5 |
| FN0.5 | 0.5 | FN10 | 10 |
| FN1 | 1 | FN100 | 100 |
| FN2 | 2 | FNM50 | 50 |

*Note*. FN indicates the co-precipitated samples and FNM indicates the mechanically mixed one.

the octahedral sites. There are, however, only a limited and contradictory reports available on the solid solubility of NiO in $Fe_2O_3$ (*15, 18*) and no detailed informations on the structural and electrical properties of the system $Fe_2O_3$–NiO with lower concentrations of NiO are available.

In our previous papers (*19–21*) thermal transformations of the hydrated ferric oxide gel and the iron–nickel mixed oxide gels prepared by hydroxide co-precipitation technique have been reported. In this paper the solid solubility of NiO in $Fe_2O_3$ and the formation of nickel ferrite under different experimental conditions are reported. The electrical properties of these samples have been investigated and are communicated separately (*22*).

**Experimental Procedure**

Ferric oxide, nickel oxide, and iron–nickel mixed oxide samples were prepared from the corresponding hydroxide samples by heating the samples in an electric furnace for a soaking time of 1 hr. The hydroxide samples were prepared from analytical grade nickel nitrate, ferric ammonium sulfate, and sodium hydroxide as reported earlier (*21*). The sample code and the amount of NiO present in each of the samples are given in Table I.

The samples were first heated to 550°C for complete conversion to oxides and then were pressed into pellets of around 12 mm diameter and 3 mm thickness in a hydraulic press under a pressure of 35,000–40,000 psi. The pellets were sintered in an electric furnace in the temperature range 1050–1300°C for 4 hr. After sintering, the samples were allowed to cool inside the furnace. However, the power to the furnace was controlled in such a way that a faster cooling rate (8–10°C/min) was obtained within the temperature range 600–1000°C. The sintered specimens were reground and the powdered samples were used for the following experiments.

Infrared spectra of the oxide samples were taken with a grating infrared spectrophotometer Model-577 (Perkin–Elmer) in the range 4000–200 $cm^{-1}$ with CSI film technique. The sample to CSI ratio was 1 : 100–200.

The magnetic susceptibility of the samples was measured with a Gouy balance at room temperature. Well-powdered samples were tightly packed in the Gouy tube of around 12 cm in length and 0.8 to 1.0 cm diameter (made of fused silica), which was suspended in between the poles of the magnet in such a way that a part of the sample was in the magnetic field of high intensity while the other portion was in a negligible field. The field strength was 5.5 kOe and the mercuric cobalt thiocyanate powder was used to standardize the balance. As the magnetic susceptibilities of most of the samples were very high, the samples were sufficiently diluted with alumina.

Phase analysis of the specimens was carried out with DRON II (USSR) X-ray diffractometer using iron radiation with a power rating of 30 kv and 15 ma. A scanning rate of 2°/min was used for this purpose.

Diffraction patterns obtained by Debye–Scherrer technique were used for the calculation of the lattice parameters. A Debye–
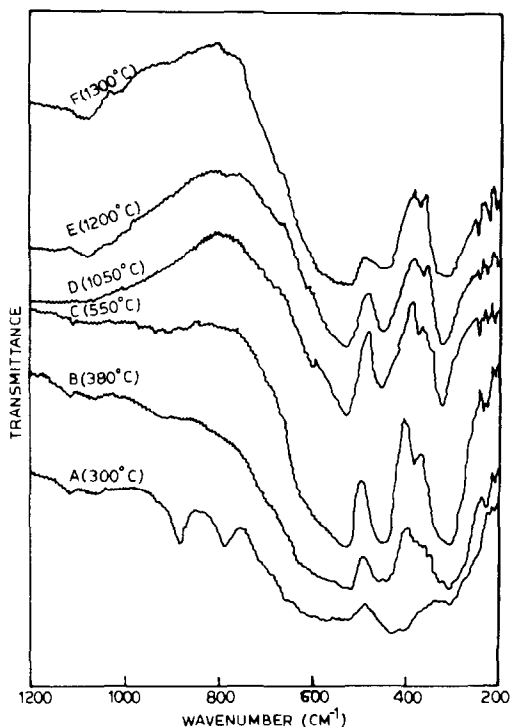
Scherrer camera of 11.46 cm diameter and CrKα radiation were used for this purpose. An exposure time of 10–12 hr was necessary to obtain sufficiently intense pattern. Precise lattice parameters were calculated by a least-square method using a computer program.

## Results

Infrared spectra of hydrated ferric oxide gel heated to different temperatures (300–1300°C) are given in Fig. 1. Curve A indicates the presence of two well-defined peaks around 900 and 800 cm⁻¹ due to the O–H · · · O bending vibrations of α-FeOOH and has been explained earlier (19). In addition to these, the curve shows the presence of other peaks in the frequency region of 600–200 cm⁻¹. These

peaks, however, are very broad and it is difficult to locate their exact positions. When the gel is heated above 300°C, the absorption peaks in the region are comparatively clear and better developed (curves B–F). In curves B and C the peak positions are found to be almost the same (525, 450, and 305 cm⁻¹) but the same peaks have shifted to 532, 455, and 325 cm⁻¹, respectively, for the sample sintered at 1050°C (curve D). In curve C the intensities of the three strong peaks (525, 450, and 305 cm⁻¹) are almost the same but in curve D the middle peak (455 cm⁻¹) has a lesser intensity than the other two (532 and 325 cm⁻¹). With further increase of sintering temperature (1200 and 1300°C) there is practically no change in the peak positions compared to that of curve D but the peak shape and size have changed appreciably. Particularly the peaks of the sample sintered at 1300°C (curve F) are more diffused and broadened.

The infrared spectra of the iron–nickel mixed oxides, containing up to 10 mole% of NiO, either heated to 550 or sintered at 1050°C are given in Figs. 2 and 3, respectively. The absorption spectra of the nickel oxide, which has been obtained by heating the nickel hydroxide at 550°C is also indicated in Fig. 2. It may be seen that with increasing concentration of NiO the peaks are slightly shifted toward lower frequencies (Fig. 2). The intensities of the absorption also decrease gradually with increase of concentration of NiO. The sample FN100 shows a very broad peak around 420 cm⁻¹. Figure 3 indicates that with 0.5 mole% of NiO the peaks of the ferric oxide get shifted to higher frequencies. For instance, the band at 532 cm⁻¹ of the α-Fe₂O₃ has been shifted to 545 cm⁻¹. With further increase of NiO, the peaks are coming back to their original positions but beyond 5 mole% of NiO the bands once again shift to higher frequencies. Another point to be noted in Fig. 3 is that the intensity of the 380-cm⁻¹ peak, in general, decreases and it
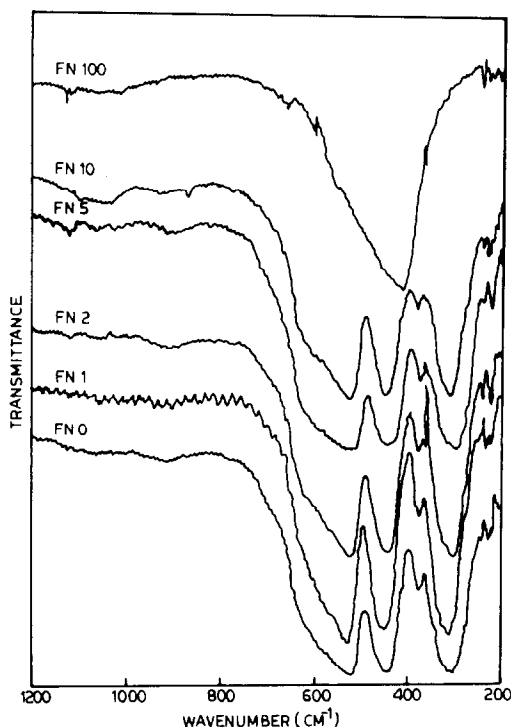
FIG. 2. Infrared spectra of iron–nickel mixed oxides containing up to 10 mole% NiO heated at 550°C.

is completely absent in the sample containing 10 mole% of NiO.

The magnetic susceptibility $(\chi_g)$ values, measured at room temperature, of the mixed oxide samples heated to 550 as well as sintered at 1050°C are plotted against nickel oxide content and are given in Fig. 4. It is observed that for the samples heated to 550°C the $\chi_g$ value remains constant at least up to 2 mole% NiO followed by a very sharp rise. On the other hand, the susceptibility increases almost linearly with NiO content when the samples are sintered at 1050°C.

The lattice parameters ($a$ and $c$), $c/a$ ratio, and the unit cell volume of the mixed oxide samples heated to 550°C as well as of those sintered at 1050 and 1200°C are given in Figs. 5 through 7. The lattice constants and the volume of the unit cell decrease up

to 2 mole% of NiO (Fig. 5) beyond which the values gradually increase. Similar trend is also observed in Figs. 6 and 7 but the nickel oxide concentrations corresponding to the minimum values are only 1.0 and 0.5 mole%, respectively, in these cases. A continuous increase of $c/a$ value up to 2 mole% NiO is observed in Figs. 6 and 7 but in Fig. 5 the ratio passes through a minimum at 0.5 mole% of NiO.

## Discussion

The variation in the shape and intensity of the infrared spectra of the ferric oxide formed by heating the ferric oxide gel to different temperatures (300–1300°C) may be due to the increase of crystallinity of the ferric oxide formed. The X-ray diffraction
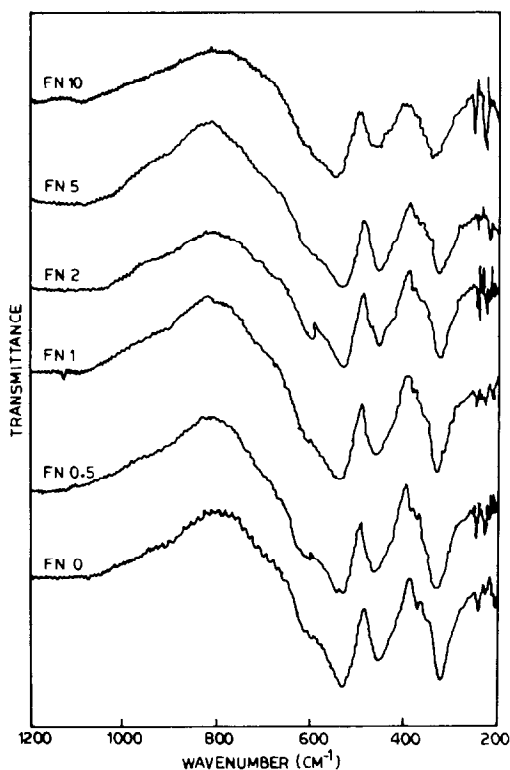


FIG. 3. Infrared spectra of iron–nickel mixed oxides containing up to 10 mole% of NiO sintered at 1050°C.
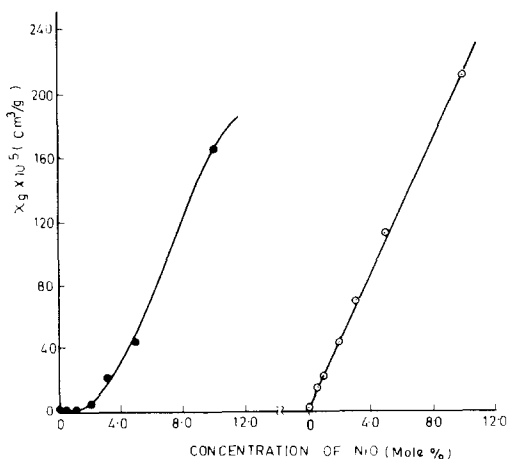
FIG. 4. Magnetic susceptibility of iron–nickel mixed oxides: heated at 550°C (●) and sintered at 1050°C (○).

studies show that the oxide formed is α-Fe$_2$O$_3$ above 300°C and therefore the bands in the oxide region can be assigned to the different vibration frequencies of α-Fe$_2$O$_3$. The infrared spectra of α-Fe$_2$O$_3$ can be assigned to two groups (4). One set involving

the oxygen vibrations relative to stationary cation sublattice and the other set is due to the vibrations of the cations relating to each other, in which oxygen undergoes adjustments to give minimum changes in cation–oxygen distance.

As given in Table II discrepancies exist in the reported location of the characteristic infrared absorption bands of α-Fe$_2$O$_3$. The spectra, to a large extent, depends on the method of preparation and the other experimental conditions. The differences observed in positions and intensities of the different peaks between the samples heated to 550°C and those sintered at 1050°C in the present investigation (Fig. 1, Table II) are probably due to a considerable increase in the size of the α-Fe$_2$O$_3$ grains above 1000°C. It is reported (5, 27) that the sintering of α-Fe$_2$O$_3$ takes place only above 900°C and the crystallite size increases to many micrometers above this temperature. Yariv and Mendelovici (5) have given the name proto-hematite for the poorly crystalline α-Fe$_2$O$_3$
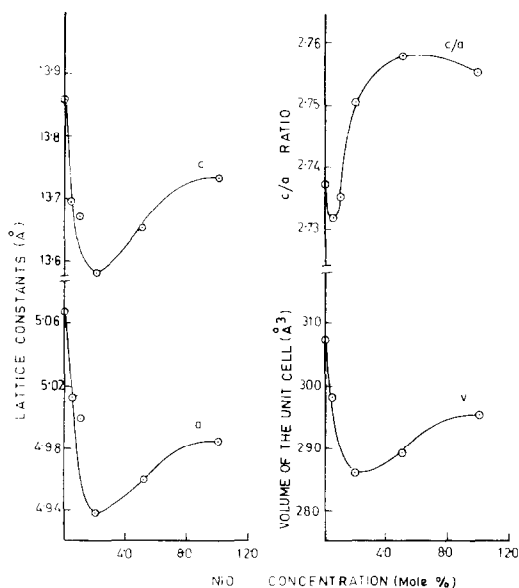


FIG. 5. Variation of the lattice parameters (a,c), c/a ratio, and unit cell volume with the nickel oxide content of the samples heated at 550°C.
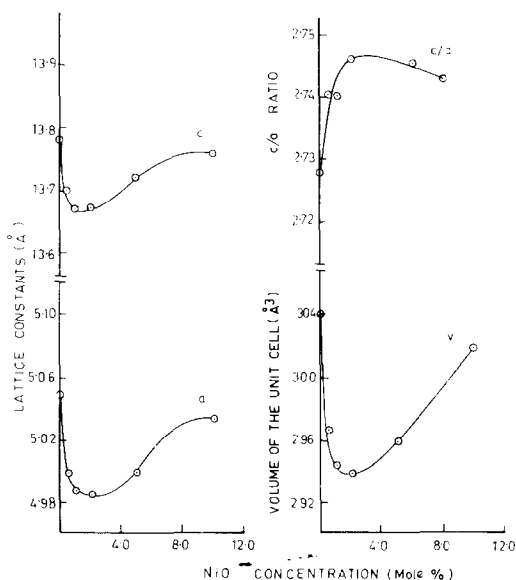


FIG. 6. Variation of lattice parameters (a,c), c/a ratio, and volume of unit cell with the nickel oxide content of the samples sintered at 1050°C.
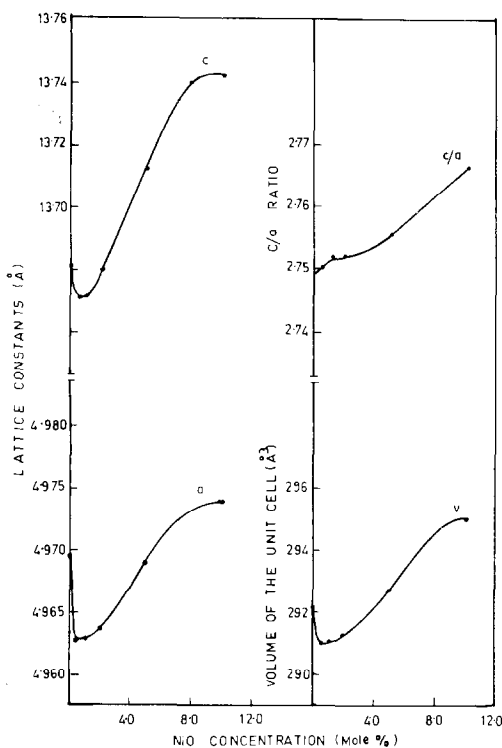
FIG. 7. Variation of lattice parameters $(a,c)$, $c/a$ ratio, and volume of the unit cell with the NiO content of the samples sintered at 1200°C.

molecules and hematite for the well crystalline and perfectly ordered ones. The broadened and more diffused bands observed for $\alpha$-$Fe_2O_3$ sample sintered at 1200 and 1300°C (Fig. 1) arise from continuous absorption of energy by the mobile electrons formed by the loss of lattice oxygen. The presence of both $Fe^{2+}$ and $Fe^{3+}$ ions in the octahedral sites increases the exchange of electrons between these ions resulting in a continuous absorption of energy.

The gradual decrease of intensity as well as the frequencies of the absorption spectra of all mixed oxides heated to 550°C with increasing concentration of NiO (Fig. 2) is explained on the basis of increased concentration of nickel ferrite, which has two broad peaks (28) in the same frequency region (600–200 $cm^{-1}$) as that of $\alpha$-$Fe_2O_3$.

Such a view is also supported by the results obtained on the mechanically mixed sample containing 50 mole% of NiO heated to 550°C. The X-ray diffraction result of the mechanically mixed sample shows a considerable quantity of nickel ferrite along with $\alpha$-$Fe_2O_3$. The infrared spectrum of the sample shows three strong absorption peaks (Fig. 8) similar to that of pure $\alpha$-$Fe_2O_3$ (Fig. 1) at 520, 435, and 305 $cm^{-1}$. In this sample the peak at 435 $cm^{-1}$ is having slightly higher intensity than that of the other two peaks (520 and 305 $cm^{-1}$) and the peak at 380 $cm^{-1}$ has almost disappeared. The absence of 380 $cm^{-1}$ peak is an indication for the presence of nickel ferrite. Similar explanation was earlier put forward by Gillot et al. (29) to indicate the presence of $ZnFe_2O_4$ along with $\alpha$-$Fe_2O_3$.

The observed shift in peak positions of $\alpha$-$Fe_2O_3$ with the addition of 0.5 mole% of NiO when the mixed oxide samples are sintered at 1050°C (Fig. 3) is attributed to the substitution of $Ni^{2+}$ ions for $Fe^{3+}$ ions in $\alpha$-$Fe_2O_3$ lattice. In the oxide samples the cation–oxygen vibrational frequencies depend on (i) the mass of the cation, (ii) the metal–oxygen bonding strength, (iii) cation electronic structure, and, to a certain extent,

TABLE II

Peak Positions in Infrared Spectra of $\alpha$-$Fe_2O_3$ Heated to Different Temperatures along with the Values Reported by Different Investigators

| Peak positions ($cm^{-1}$) | | | | | | References |
|---|---|---|---|---|---|---|
| 600 (shoulder) | 525 | 450 | 380 | 310 | — | (550°C)[a] |
| 600 | 532 | 455 | 375 | 325 | — | (1050°C)[a] |
| — | 530 | 450 | 370 | 325 | — | (1200°C)[a] |
| — | 530 | 450 | 375 | 320 | — | (1300°C)[a] |
| — | 560 | 468 | 370 | 325 | — | (23) |
| — | 532 | 449 | 391 | 312 | — | (24) |
| — | 540 | 470 | — | 345 | — | (25) |
| 580 | 520 | 475 | — | — | — | (26) |
| — | 530 | 445 | — | 308 | 273 | (5) |
| — | 543 | 468 | — | 333 | — | (5) |

[a] Present investigation. The sintering temperatures of the samples are mentioned in parentheses.
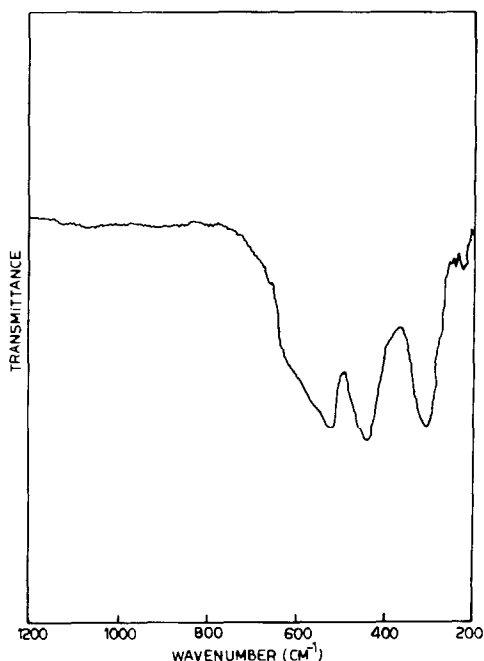
FIG. 8. Infrared spectra of FNM50 heated to 550°C.

(iv) on the chemical nature of the neighboring atoms. Therefore, when a cation is replaced by another cation, all these parameters are simultaneously modified and there are shifts in the peak positions (30). The gradual decrease of frequencies in the case of samples FN1 and FN2 and the reverse trend observed in the sample containing more than 5 mole% of NiO is interpreted in terms of the formation of nickel ferrite and its interaction with the excess $\alpha$-Fe$_2$O$_3$, respectively.

The magnetic susceptibility ($\chi_g$) values of $\alpha$-Fe$_2$O$_3$ and NiO heated at 550°C are found to be very close to each other (26 × 10$^{-6}$ and 44 × 10$^{-6}$ cm$^3$/g, respectively). Therefore, the formation of a solid solution between these two oxides may not change the $\chi_g$ values to a significant extent. This has been found to be the case in the samples containing up to 2 mole% of NiO heated at 550°C (Fig. 4). An almost linear variation of $\chi_g$ value with nickel oxide content above 2

mole% of NiO indicate that there is a continuous increase of nickel ferrite at higher concentrations of NiO. When the samples are sintered at 1050°C the increase of the magnetic susceptibility is much more significant and in this case the linearity is observed from the very beginning, probably indicating that there is a decrease in solubility of NiO in Fe$_2$O$_3$ lattice with increase of sintering temperature.

The X-ray diffraction results of mixed oxide samples heated to 550°C as well as sintered at 1050 and 1200°C show an initial decrease of lattice parameters and unit cell volume (Figs. 5–7). Substitution of Ni$^{2+}$ ions for Fe$^{3+}$ ions in the $\alpha$-Fe$_2$O$_3$ lattice may lead to an increase in the lattice constants because the reported ionic radius of Ni$^{2+}$ ion is 0.69 Å in the octahedral site which is found to be slightly more than that of Fe$^{3+}$ ion (0.65 Å) in the same site. On the contrary, we observed a decrease in their values which can be explained in the following way.

When a divalent Ni$^{2+}$ ion is substituted for Fe$^{3+}$ ion, the charge compensation can be accomplished by (i) either generation of holes in the lattice or (ii) generation of structural defects like cation interstitial and anion vacancies.

The possibility of cation interstitial can be ruled out as it will increase the lattice constants to a larger extent which has not been found in this case. On the other hand, formation of oxygen vacancies decreases the lattice constants and hence the volume of the unit cell. In fact, both oxygen vacancies and electron holes are formed simultaneously when Fe$^{3+}$ is substituted by Ni$^{2+}$ as discussed elsewhere (22). These electron holes are usually localized either at the Fe$^{3+}$ or Ni$^{2+}$ sites converting some of these ions to Fe$^{4+}$ and Ni$^{3+}$, respectively. The radii of both the later ions are smaller than those of the former. As a result, the formation of electron holes may also lead to a decrease in the lattice constants of $\alpha$-Fe$_2$O$_3$. It may,

therefore, be concluded that the decreasing effect on the lattice constants is due to the simultaneous presence of oxygen vacancies and electron holes. This decreasing effect is much greater than the increasing effect due to larger ionic radius of $Ni^{2+}$ ions and may, therefore, be considered as due to the formation of solid solution. Similar results of simultaneous presence of both holes and oxygen vacancies have been reported by many investigators (31) when lower valency cation is substituted for higher valency cations.

It is interesting to note that the lattice constants of the $Fe_2O_3$ at each sintering temperature goes through a minimum with increasing NiO content. Even though the exact value of NiO corresponding to this minimum is different for different temperatures, the increase in lattice constants beyond this minimum is attributed to a decrease in solid solubility at higher concentrations of NiO. Such an effect has been earlier detected by Kennedy et al. (32) in $CeO_2$–$\beta$-$Al_2O_3$ system. The decreasing solid solubility at a higher concentration is also associated with the formation of the nickel ferrite phase as indicated by the appearance of a few distinct X-ray diffraction lines particularly those corresponding to (220), (400), and (440) planes of the Ni $Fe_2O_4$. It may therefore be assumed that the formation of the nickel ferrite phase is responsible for the observed decrease in solid solubility.

From the positions of the minima in the variations of the lattice parameters, it may be concluded that the maximum solubility of NiO in $\alpha$-$Fe_2O_3$ also decreases with increasing sintering temperature. For example, the solubility is around 2 mole% when the samples are heated to 550°C but it is found to be only 1 and 0.5 mole% when the samples are sintered at 1050 and 1200°C, respectively. In the last case the solubility may be even less than 0.5 mole%. How-

TABLE III

LATTICE CONSTANTS, $c/a$ RATIO, AND UNIT CELL VOLUME OF FN0 SAMPLE HEATED TO DIFFERENT TEMPERATURE

| Temperature (°C) | $a^a$ (Å) | $c^a$ (Å) | $c/a$ | $V$ (Å)³ |
|---|---|---|---|---|
| 550 | 5.054 | 13.859 | 2.742 | 306.6 |
| 800 | 5.055 | 13.809 | 2.732 | 305.6 |
| 1050 | 5.049 | 13.778 | 2.729 | 304.2 |
| 1100 | 5.035 | 13.754 | 2.732 | 302.0 |
| 1200 | 4.969 | 13.650 | 2.749 | 291.9 |
| ASTM value | 5.034 | 13.752 | 2.732 | 301.8 |

$^a$ Error limit is ±0.001 Å.

ever, the same could not be ascertained since the lowest quantity of NiO used in our samples was 0.5 mole%. The $c/a$ ratio of the samples shows an increase with increase of nickel oxide content up to 5 mole% (Figs. 5–7), which indicates that there is a non-uniform variation of "$a$" and "$c$" values with increase of concentration of NiO.

The X-ray diffraction results of $\alpha$-$Fe_2O_3$ sample heated to 550°C show significantly higher lattice constant values (as well as $c$) compared to that of ASTM values (Table III). However, the values decrease as the sample is heated to higher temperatures. The "$a$" and "$c$" values are found to be almost the same as those of the standard ones when the sample is sintered at 1100°C. The 1200°C sintered sample shows significantly lower value than those of the standard ASTM values. These observations of change in lattice parameters with increase of heating temperature is due to the increase of particle size. The finer particles have been reported to possess higher lattice constants (33). The lower "$a$" and "$c$" values of $\alpha$-$Fe_2O_3$, when sintered at 1200°C, are due to the loss of lattice oxygen which creates a number of oxygen vacancies in $\alpha$-$Fe_2O_3$ lattice.

## References

1. R. F. G. GARDNER, F. SWEET, AND D. W. TAN-NER, *J. Phys. Chem. Solids* **24**, 1183 (1963).
2. A. J. BOSMAN AND H. J. VAN DAAL, *Advan. Phys.* **19**, 1 (1970).
3. J. H. DE WIT, A. F. BROERSMA, AND M. STRO-BAND, *J. Solid State Chem.* **37**, 242 (1981).
4. V. C. FARMAR, "The Infrared Spectra of Miner-als," p. 183, Mineralogical Society, London (1974).
5. SH. YARIV AND E. MENDELOVICI, *Appl. Spec-trosc.* **33**, 410 (1979).
6. O. V. KRYLOV, "Catalysis by Nonmetals," Aca-demic Press, New York (1970).
7. K. H. HELLWEGE AND A. M. HELLWEGE, eds., "Magnetic Oxides and Related Compounds," Part b, 111/12b, p. 7, Springer-Verlag, Berlin (1980).
8. R. J. DENNARD AND W. L. KEHL, *J. Catal.* **21**, 282 (1971).
9. V. P. SHCHUKIN, S. A. VEN'YAMINOV, AND G. K. BORESKOV, *Kinet. Katal.* **11**, 547 (1971).
10. R. S. MANN AND M. K. DOSI, *J. Catal.* **28**, 282 (1973).
11. R. MALINSKI, M. AKIMOTO, AND E. ECHGOYA, *J. Catal.* **44**, 101 (1976).
12. H. E. VON STEINWEHR, *Z. Kristallogr.* **125**, 377 (1967).
13. G. H. GEIGER AND J. B. WAGNER, JR., *Trans. Metall. Soc. AIME* **233**, 2092 (1965).
14. D. CORMACK, R. F. G. GARDNER, AND R. L. MOSS, *J. Catal.* **17**, 219 (1970).
15. D. CORMACK, D. A. POYNTER, C. J. BURLACE, AND R. L. MOSS, *J. Catal.* **19**, 135 (1972).
16. B. MANI, V. SITAKARA RAO, AND H. S. MAITI, *J. Mater. Sci.* **15**, 925 (1980).
17. H. L. SANCHEZ, H. STEINFINK, AND S. WHITE, *J. Solid State Chem.* **41**, 90 (1982).
18. J. S. CHOI AND YOON, *J. Phys. Chem.* **74**, 1095 (1970).
19. S. RAJENDRAN, V. SITAKARA RAO, AND H. S. MAITI, *J. Mater. Sci.* **17**, 2709 (1982).
20. S. RAJENDRAN, V. SITAKARA RAO, AND H. S. MAITI, *Trans. Indian Ceram. Soc.* **41**, 97 (1982).
21. V. SITAKARA RAO, S. RAJENDRAN, AND H. S. MAITI, submitted for publication.
22. H. S. MAITI, S. RAJENDRAN, AND V. SITAKARA RAO, in press.
23. N. T. McDEVITT AND W. L. BAUN, *Spectrochim. Acta* **20**, 799 (1964).
24. H. C. LIESE, *Amer. Mineral.* **52**, 1198 (1967).
25. U. SCHWERTMANN AND R. M. TAYLER, "Miner-als in Soil Environment," p. 145, Soil Science So-ciety of America Inc., Madison (1977).
26. M. P. BOGDANOVICH, YU. P. VOROBEV, A. M. MEN, A. V. SEREBRYAKOVA, AND G. I. CHU-FAROV, *Opt. Spectrosk.* **29**, 1151 (1970).
27. H. P. ROOKSBY, "The X-ray Identification and Crystal Structures of Clay Minerals," p. 354, Min-eralogical Society, London (1961).
28. R. D. WALDRON, *Phys. Rev.* **99**, 1727 (1955).
29. B. GILLOT, R. M. BENLOUCIF, AND A. ROUSSET, *J. Solid State Chem.* **39**, 329 (1981).
30. J. PREUDHOMME AND P. TARTE, *Spectrochim. Acta A* **27**, 845 (1971).
31. H. YAMAMURA, H. HANEDA, S. SHIRASAKI, AND K. TAKADA, *J. Solid State Chem.* **36**, 1 (1981).
32. J. H. KENNEDY, A. M. SCHULER, AND G. E. CA-BANISS, *J. Solid State Chem.* **42**, 170 (1982).
33. N. YAMAMOTO, *J. Phys. Soc. Jpn.* **24**, 25 (1968).